

PROCEEDINGS OF SPIE

[SPIEDigitallibrary.org/conference-proceedings-of-spie](https://www.spiedigitallibrary.org/conference-proceedings-of-spie)

In-situ testing of organic photovoltaic (OPV) modules to examine modes of degradation in an arid-hot climate

Chief, Manuelito, Boyer, Kyle, Simmons-Potter, Kelly

Manuelito Chief, Kyle Boyer, Kelly Simmons-Potter, "In-situ testing of organic photovoltaic (OPV) modules to examine modes of degradation in an arid-hot climate," Proc. SPIE 11474, Organic, Hybrid, and Perovskite Photovoltaics XXI, 114741O (21 August 2020); doi: 10.1117/12.2568685

SPIE.

Event: SPIE Organic Photonics + Electronics, 2020, Online Only

In-situ testing of organic photovoltaic (OPV) modules to examine modes of degradation in an arid-hot climate

Manuelito Chief^{*a}, Kyle Boyer^a, Kelly Simmons-Potter^a

^aDept. of Electrical and Computer Engineering, University of Arizona, 1230 E Speedway Blvd., Tucson, AZ USA 85719

ABSTRACT

The AzRISE-TEP Solar Test Yard is a 600-module capacity test bed that provides the environment for in-situ testing of PV module performance, with real-time data collection of module power production and local weather conditions. This work involves the examination of flexible, semi-transparent, organic photovoltaic (OPV) modules in an outdoor testing environment to study degradation in the hot, arid, Tucson, AZ climate. The work reports on changes in the I-V performance and efficiency of a string of two OPV modules in order to estimate degradation experienced by the OPV modules. The study finds that the module string under test dropped to below 80% of its initial power conversion efficiency (PCE) after 54.58 days, and predicts that the PCE will drop below 50% of its initial state after 114.53 days from deployment.

Keywords: Organic Photovoltaics, OPV, degradation, field testing, reliability, outdoor

1. INTRODUCTION

Organic photovoltaics (OPV) are gaining traction in many use cases where the more efficient Si based PV (SiPV) modules are not practical¹. Their transparency to broad spectral wavelength windows makes them particularly useful for applications which require both electrical power and light transmission, such as in building-integrated applications and in greenhouses². Further, their mechanical flexibility and light weight enables them to be more easily deployed than traditional SiPV on curved surfaces, on the roofs of irregularly shaped buildings, and in applications for which heavy module support framework is not feasible.

A major limitation of OPV modules, however, is their long-term stability. Degradation in OPV modules has been observed to result from exposure to oxygen, moisture, temperature, ultraviolet (UV) radiation, and mechanical stress^{2,3}. Mechanical stress is particularly problematic for flexible OPV modules, because repeated stretching or bending can damage metallic contacts, and can cause encapsulation layers to separate from underlying OPV material layers⁴. Moreover, UV exposure can lead to cracking in laminate layers⁴. Such encapsulation delamination and cracking allow moisture and oxygen to easily diffuse into the OPV layered device structure, resulting in water and oxygen coming into contact with the metallic contacts and with the organic semiconductor layers, leading to oxidation and corrosion of the materials. Oxidation of the semiconductor layers reduces efficiency by hindering charge transport, introducing trap states, and altering the optical properties of the material³. Oxidation of the contacts can prevent charge extraction, leading to reduced efficiency and, eventually, to total device failure. The points where external wires attach to the module are particularly vulnerable to this type of damage, due to the fact that there is necessarily a hole in the encapsulation layer at the point where the electrical connection is made.

These degradation-causing mechanisms are prevalent in outdoor conditions. A number of studies have been performed to examine the behavior and stability of OPV modules in outdoor environments, many utilizing bulk-heterojunction (BJH) P3HT:PCBM or MEH-PPV:PCBM modules. One such effort which focused on P3HT-PCBM OPVs, found that after two years the modules still produced over 80% of their initial Maximum Power Point (MPP) power⁵. Another study, conducted simultaneously in four different climates, found that the module lifetimes vary greatly depending on temperature and how well electrical contacts are sealed⁶.

In the current paper, an outdoor reliability study of a commercially available, flexible, semi-transparent OPV is carried out in a hot-arid climate (Tucson, AZ). This study analyzes the performance of two commercially available OPV modules that utilize a PBTZT-stat-BDTT-8 based solution for the electron donor material. The performance of these modules over a three-month, field-based operation is monitored and discussed.

^{*}manuelitochief@email.arizona.edu

2. EXPERIMENTAL

2.1 Testing Facility

The AzRISE-TEP Solar Test Yard is a 600-module capacity test bed in Tucson, AZ that enables in-situ testing of PV module performance, with real-time data collection of module power production and local weather conditions. The testing facility utilizes two on-site weather stations, the Mast-Affixed Weather Station (MAWS) and Smart Solar Field (SOFIE) units^{7,8}. Local weather data collected from MAWS for the current study provided global horizontal irradiance (GHI), plane of array (POA) irradiance, humidity, ambient temperature, rainfall, wind velocity, and wind direction. Weather data was taken once per minute using a Campbell Scientific CR1000 datalogger. The GHI, humidity, ambient temperature, rainfall, wind velocity, and wind direction sensors were mounted on a mast unit while two irradiance sensors (GHI and POA) were mounted on an adjacent solar rack.

2.2 Outdoor Testing

The organic photovoltaics modules used in this study are commercially available, semi-transparent and flexible organic photovoltaic modules. The OPV modules are based on a PBTZT-stat-BDTT-8 solution, similar to modules tested by Magadley et al.¹ Under Standard Test Conditions (STC), the modules under test have a short circuit current (I_{sc}) of 0.72 A, open circuit voltage (V_{oc}) of 24 V, max power current (I_{mpp}) of 0.48 A, max power voltage (V_{mpp}) of 16 V, and max power (P_{mpp}) of 7.6 W. Each of the OPV modules has a total area of 0.8 m x 1.0 and an active area (A_{pv}) of 0.655 m x 0.855 m. For the experimental results reported here, the electrical characteristics of a string of two modules, connected in parallel and laminated by the manufacturer into a single OPV roll, were monitored.

The OPV module string under test was stored in a darkened laboratory space at approximately 20°C prior to installation at the outdoor test yard. In order to perform studies in the outdoor, in-situ, environment, the OPV modules were affixed to a polycarbonate sheet that is commonly used in greenhouse glazing applications (Lexan Thermoclear multi-wall polycarbonate sheet) and placed on a fixed-tilt south-facing rack with a tilt equal to the latitude angle (32°N) as shown in Fig. 1. Current-voltage measurements were taken using a Keithley 2420 SMU in a four-wire measurement configuration every two minutes between 8 AM and 4 PM. Each I-V curve was swept from 0 V to V_{oc} in increments of 100 mV. A Keithley 2000 Multimeter was used to determine the open circuit voltage for each measurement sweep, and a LabVIEW program was used to automate the I-V measurements. In between I-V measurements, the modules were kept under open circuit conditions. To monitor module temperature, six type-T thermocouples were attached to the back of the modules. The back-of-panel temperature was collected every 30 seconds using a Campbell Scientific CR1000 data logger.



Figure 1. OPV modules installed in the AzRISE-TEP Solar Test Yard.

2.3 Temperature Dependence Characterization

In order to characterize the effect of temperature on the OPV electrical characteristic and to establish temperature derating coefficients for voltage, current, power, and efficiency of the modules, a single, identical, OPV module was placed inside a controlled environmental test chamber located in our University of Arizona laboratories⁸⁻¹⁰. The OPV module was tested under 1000W/m² full solar spectrum irradiance. Two type-T thermocouples were placed in direct contact with the back of the module to monitor cell temperature while the test chamber was set for internal temperatures ranging from 5°C to 45°C in steps of 10°C. A 5-minute ramp time was sufficient to enable the stable transition between chamber temperatures during the test cycle, and a 10 min soak at each temperature allowed a total of four I-V measurements to be made at each temperature. The OPV parameters of V_{oc} , I_{sc} , P_{mpp} were taken from the I-V curves and compared against the cell temperature to determine temperature de-rating coefficients at STC. The measured temperature coefficients are given in Table 1. As seen, I_{sc} , V_{oc} and P_{max} have a decreasing performance with increasing temperature. Additionally, V_{oc} and P_{max} show a stronger de-rating effect than I_{sc} .

Table 1. Measured temperature de-rating coefficients.

	Temperature Coefficient ($\gamma_{x,dc}$)
P_{max}	-0.0416 W/°C
V_{oc}	-0.0483 V/°C
I_{sc}	-0.0012 A/°C

2.4 Data Analysis

The OPV outdoor performance degradation following its installation in the test yard was characterized by analyzing the collected I-V curve data. Measurements were taken between the period of 8 AM to 4 PM solar time and electrical quantities (V_{oc} , I_{sc} , and P_{mpp}) of the module string were determined for each time period. Irradiance data collected from the co-located weather stations was used in combination with temperature derating coefficient information in order to correct all data to STC. Equations 1 to 3 show the correction method used, in which the quantities subscripted “stc” are the corrected STC values, those subscripted “measured” are the measured data values, $\gamma_{x,dc}$ are the temperature derating coefficients given for power, voltage, and current in Table 1, T_{mod} is the measured module backside temperature, and T_{ref} is the STC reference temperature of 25°C.

$$V_{stc} = V_{oc,measured} - (\gamma_{vdc.}) * (T_{mod} - T_{ref}) \quad (1)$$

$$I_{stc} = I_{oc,measured} - (\gamma_{idc.}) * (T_{mod} - T_{ref}) \quad (2)$$

$$P_{stc} = P_{measured} - (\gamma_{pdc.}) * (T_{mod} - T_{ref}) \quad (3)$$

The POA irradiance (E) data from MAWS was used to calculate power conversion efficiency (PCE) of the module string as shown in equation 4. Daily time windows during which the incident solar irradiance ranged between 800 W/m² and 1100 W/m² were identified and daily I-V data collected during those time windows was analyzed in order to monitor changes in the overall performance of the OPV module string from day-to-day. The focus on data selection and analysis under the above irradiance conditions (roughly between the hours of 8 AM and 4 PM) reduced data noise that can result from low ambient light levels, thus minimizing error in the time-dependent efficiency analysis. The fill factor (FF) under STC was found using P_{max} , I_{sc} , and V_{oc} as shown in equation 5.

$$\eta_{stc}(PCE) = \frac{P_{max,stc}}{E * A_{PV}} = \frac{I_{sc}V_{oc}FF}{E * A_{PV}} \quad (4)$$

$$FF = \frac{P_{max}}{I_{sc}V_{oc}} \quad (5)$$

3. RESULTS AND DISCUSSION

Figure 2 shows raw data (not corrected to STC) of an I-V curve taken after six days of deployment (4/16/2020 at 12:40 PM). Notably, the data are collected in-situ with the module string in an ambient temperature environment (air temperature = 27.1°C, module backside temperature = 54.2°C for the data shown in Fig. 2). Application of equations 1-3 enabled removal of the temperature effects from the IV curve and the STC corrected V_{oc} , I_{sc} , P_{max} , and PCE of the module string was then evaluated over the course of the full test day. Figure 3 depicts the effect of removal of temperature derating from the raw voltage, current, and maximum power data. Clear in the figure is the significant impact of temperature on the open circuit voltage for the module string. Also evident is the anticipated decrease in module string efficiency at mid-day, as both the ambient and the module backside temperatures increase.

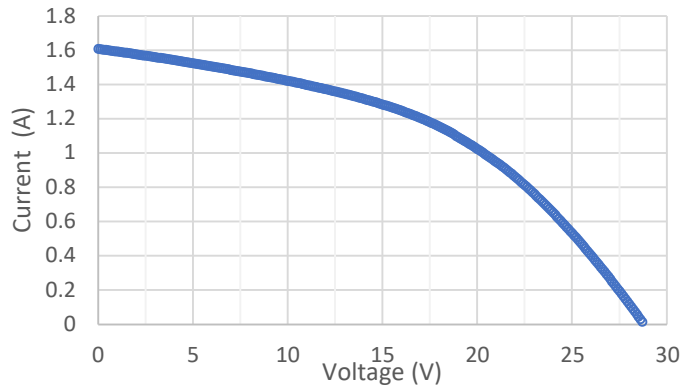


Figure 2. Representative IV Curve taken 4/16/2020 at 12:40 PM, $P_{max} = 20.82$ W, $V_{oc} = 28.80$ V, $I_{sc} = 1.61$ A, $FF = 0.45$, $T_{cell} = 54.2^\circ\text{C}$. Air temperature at time of data collection was 27.1°C.

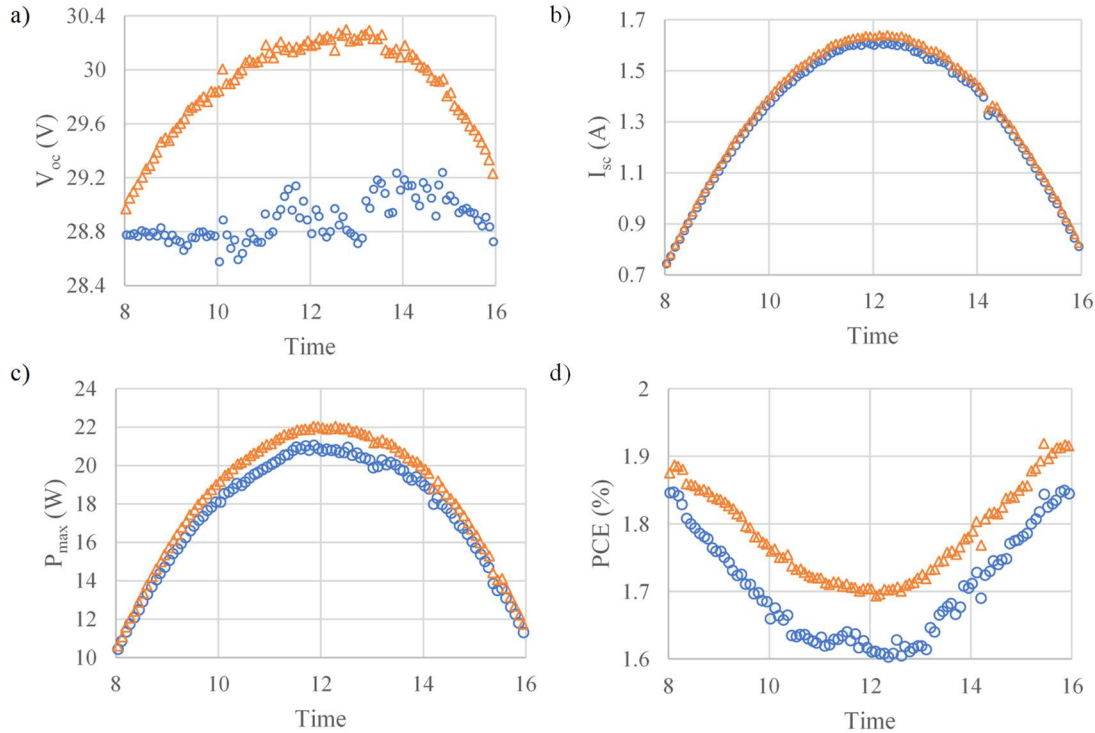


Figure 3. Module string performance over a single day (8 AM to 4 PM) in April before and after consideration of de-rating due to temperature representing (a) Voc, (b) Isc, (c) Pmax, and (d) PCE. The measured values are represented by circles. The values after considering temperature de-rating are shown by triangles.

The module performance over a three-month period (92.16 days) is depicted in Figure 4. The figure shows the P_{\max} (a) and PCE (b) for the module string during periods for which the incident solar irradiance ranged between 800 W/m^2 and 1100 W/m^2 . An examination of the data in the figure reveals that both the power and efficiency of the module string were half of their expected values for the first 4-5 days after installation. Following this initial period of poor performance, the string maximum power and efficiency increased to the anticipated average values of 20W (P_{\max}) and approximately 1.8% (PCE) respectively and remained approximately constant for nearly 18 days. This initial period of low performance was associated with maximum power point current and voltage values for the string of 0.44 Amps (I_{\max}) and 19.08 Volts (V_{\max}) respectively. In contrast, for the 18 days of higher performance condition that occurred after 6 days of installation, the maximum power point current and voltage values averaged 0.88 Amps (I_{\max}) and 18.74 Volts (V_{\max}). Given that the two OPV modules in the string are connected in parallel, the fact that the V_{\max} remains relatively constant throughout while the I_{\max} nearly doubles between the two measurement periods suggests that one of the two modules in the string initially failed to make ohmic contact with the external wires. Such a failure would prevent the photocurrent produced in one of the modules from being extracted such that it could contribute to power production of the string. It is reasonable, therefore, to propose that handling-induced stress fractures prevented current flow in half of the module string immediately after its installation at the test yard. Subsequent moderate outdoor temperatures and high module backside temperatures may have resulted in enough thermal expansion and/or flow of metal electrodes to enable ohmic contact, thus resulting in the expected performance of the OPV string after more than 5 days of installation. The steady performance of the module string between 6-18 days reflects the peak performance characteristic of the module. Interestingly, the total power produced by the string at this stage exceeds that predicted by the manufacturer at STC. This may be explained by the fact that the average irradiance the string received during this period regularly surpassed 1000 W/m^2 by 10% - 20% for several hours of each day. An examination of data for the period starting 18 days after installation reveals that both max power and PCE exhibit a steady performance degradation throughout the three-month period studied. Specifically, both metrics

display nearly linear degradation at a rate of approximately 0.45% of the initial value per day, as calculated from the linear equations fit to the data in Figures 5.

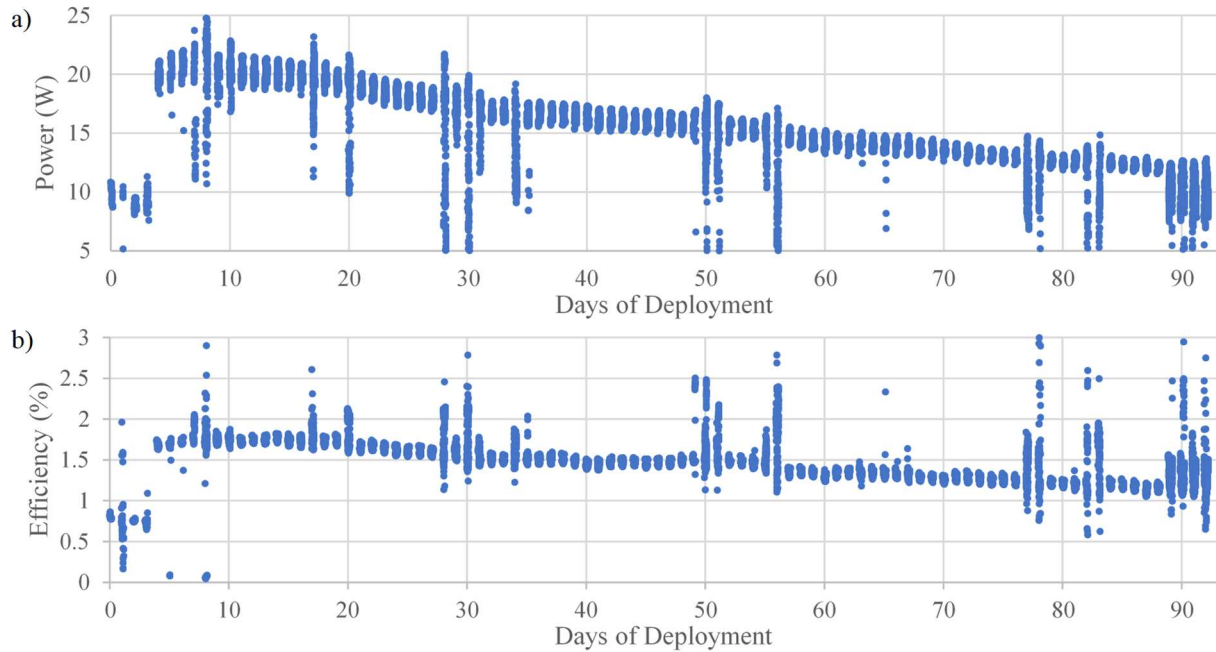


Figure 4. Module performance over a three-month period (April 10 to June 7, 24-hour days) showing (a) P_{max} and (b) PCE for irradiance levels between 800 W/m^2 and 1100 W/m^2 .

The performance of the modules can be better represented under STC with irradiance equal to $1000 \text{ W/m}^2 \pm 5 \text{ W/m}^2$, as shown in Figure 5. The figure shows the module performance parameters P_{max} (Fig. 5(a)), I_{sc} (Fig. 5(b)), PCE (Fig. 5(c)), and V_{oc} (Fig. 5(d)). As can be seen in the data, the modules show minimal performance loss between 10.1 and 17.1 days of exposure. After 17.1 days, P_{max} , I_{sc} , and PCE show a faster degradation rate that continues approximately linearly throughout the rest of the three-month test cycle reported here. During this period, P_{max} is observed to decrease by 39.4% from 19.93 W to 12.08 W. Similarly, the PCE decreases by 39.3% from 1.77 PCE to 1.08 PCE such that the overall string efficiency is at just 61.0% of the initial PCE. Analysis of the results for PCE shows the module drops below 80% of its initial efficiency after 54.58 days from deployment (T_{80}). Using a linear fit, with the equations given in Fig. 5c, for this period, the module is projected to drop below 50% of its initial PCE after 114.53 days (T_{50}). As seen in Fig. 5(b), I_{sc} decreases from 1.57 A to 1.18 A (24.8% decrease) over the period spanning 17.1 days after installation to the end of the data represented in the figure. In this same period, however, V_{oc} exhibits a slight increase in value over the three month period. Between 17.08 days and 92.16 days, V_{oc} (Fig. 5(d)) is seen to increase by 1.4% (30.9 V to 31.34 V), a value that is near the measurement error of the data. Figure 6 shows the decline in FF over the deployment period. In this case, the FF is observed to decrease from a high of 47.5 to a low of 37.5 after installation of the modules.

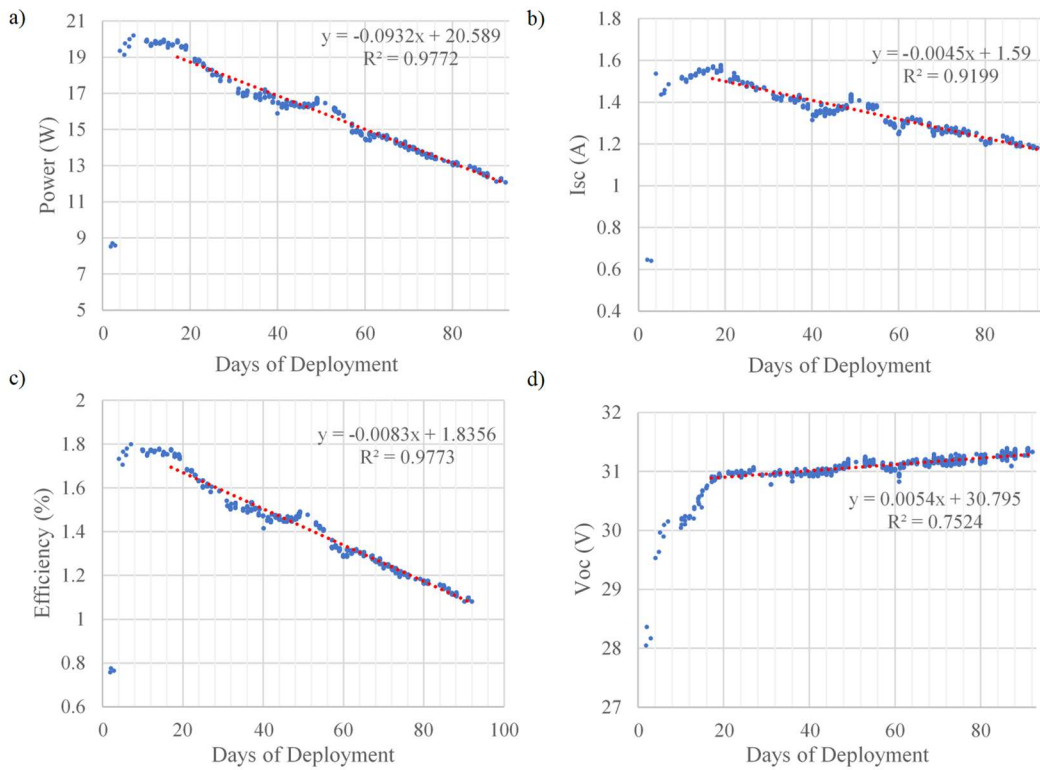


Figure 5. Module performance over a three-month period normalized to STC with irradiance equal to $1000 \text{ W/m}^2 \pm 5 \text{ W/m}^2$. Module performance is represented include (a) P_{mpp} , (b) I_{sc} , (c) PCE, and (d) V_{oc} .

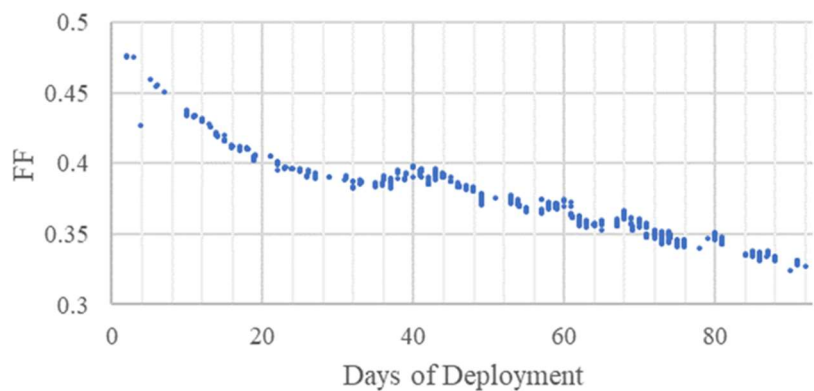


Figure 6. FF of the OPV modules at STC with irradiance equal to $1000 \text{ W/m}^2 \pm 5 \text{ W/m}^2$.

4. CONCLUSION

This study demonstrated the performance of a PBTZT-stat-BDTT-8 based, flexible, semi-transparent OPV module after three months of field-based operation in a hot, arid climate, with high levels of UV radiation. Initial results highlighted limitations in the durability of the ohmic contacts bridging the laminated module electrodes and external wiring as clear evidence suggested ohmic contact failure of one of the two modules in the string following installation. This suggests the presence of micro cracks in the ohmic connections that may have resulted from handling-induced stress. Interestingly, several days exposure to high OPV module (cell) temperatures appeared to improve the electrical connection such that the expected device performance was achieved. Following this initial poor-performance period and under the environmental conditions reported here, the OPV module string was then observed to perform as anticipated with power production approximately meeting module specifications. Prolonged exposure of the OPV string to the high temperatures and UV radiance characteristic of the field test location in Tucson, AZ resulted in a steady decline in both PV maximum power and efficiency as well as fill factor. Finally, it was observed that the module string reached its PCE T_{80} lifetime at 54.58 days and it is projected that the OPV string will reach the PCE T_{50} lifetime at 114.53 days.

5. ACKNOWLEDGEMENTS

This work was partially supported by the Arizona Research Initiative for Solar Energy (AzRISE), Tucson Electric Power (TEP), and the University of Arizona Alfred P. Sloan Foundation Indigenous Graduate Partnership. This material is based upon work supported by the National Science Foundation under Grant #DGE1735173.

REFERENCES

- [1] Berny, S., Blouin, N., Distler, A., Egelhaaf, H.-J., Krompiec, M., Lohr, A., Lozman, O. R., Morse, G. E., Nanson, L., Pron, A., Sauermann, T., Seidler, N., Tierney, S., Tiwana, P., Wagner, M. and Wilson, H., "Solar Trees: First Large-Scale Demonstration of Fully Solution Coated, Semitransparent, Flexible Organic Photovoltaic Modules," *Adv. Sci.* **3**(5), 1500342 (2016).
- [2] Magadley, E., Teitel, M., Peretz, M. F., Kacira, M. and Yehia, I., "Outdoor behaviour of organic photovoltaics on a greenhouse roof," *Sustain. Energy Technol. Assessments* **37**, 100641 (2020).
- [3] Patel, J. B., Tiwana, P., Seidler, N., Morse, G. E., Lozman, O. R., Johnston, M. B. and Herz, L. M., "Effect of Ultraviolet Radiation on Organic Photovoltaic Materials and Devices," *ACS Appl. Mater. Interfaces* **11**(24), 21543–21551 (2019).
- [4] Finn, M., Martens, C. J., Zaretski, A. V., Roth, B., Søndergaard, R. R., Krebs, F. C. and Lipomi, D. J., "Mechanical stability of roll-to-roll printed solar cells under cyclic bending and torsion," *Sol. Energy Mater. Sol. Cells* **174**, 7–15 (2018).
- [5] Angmo, D. and Krebs, F. C., "Over 2 Years of Outdoor Operational and Storage Stability of ITO-Free, Fully Roll-to-Roll Fabricated Polymer Solar Cell Modules," *Energy Technol.* **3**(7), 774–783 (2015).
- [6] Gevorgyan, S. A., Madsen, M. V., Dam, H. F., Jørgensen, M., Fell, C. J., Anderson, K. F., Duck, B. C., Mescheloff, A., Katz, E. A., Elschner, A., Roesch, R., Hoppe, H., Hermenau, M., Riede, M. and Krebs, F. C., "Interlaboratory outdoor stability studies of flexible roll-to-roll coated organic photovoltaic modules: Stability over 10,000h," *Sol. Energy Mater. Sol. Cells* **116**, 187–196 (2013).
- [7] Dzurick, M., Potter, B. G., Holmgren, W. F. and Simmons-Potter, K., "Enhanced Photovoltaic Power Model Fidelity Using On-Site Irradiance and Degradation-Informed Performance Input," 2019 IEEE 46th Photovolt. Spec. Conf., 1596–1600 (2019).
- [8] Simmons-Potter, K., Bennett, W., Fishgold, A., Potter, B. G. and Lai, T., "Data acquisition and PV module power production in upgraded TEP/AzRISE solar test yard," 23 August 2017, 13, SPIE-Intl Soc Optical Eng.
- [9] Lai, T., Potter, B. G. and Simmons-Potter, K., "Comparison of efficiency degradation in polycrystalline-Si and CdTe thin-film PV modules via accelerated lifecycle testing," *Proc. SPIE* **10370**, 20 (2017).
- [10] Lai, T., Potter, B. G. and Simmons-Potter, K., "Analysis of twelve-month degradation in three polycrystalline photovoltaic modules," *Reliab. Photovolt. Cells, Modul. Components, Syst.* **IX 9938**, 993800 (2016).